

DSS-oriented exploration of a multi-centre magnetic resonance spectroscopy brain tumour dataset through visualization

Enrique Romero¹, Margarida Julià-Sapé^{2,3} and Alfredo Vellido¹ *

1- Dept. de Llenguatges i Sistemes Informàtics - Universitat Politècnica de Catalunya
C. Jordi Girona, 1-3. 08034, Barcelona - Spain

2- Networking Research Center on Bioengineering, Biomaterials and Nanomedicine
(CIBER-BBN), Cerdanyola del Vallès, Spain.

3- Grup d'Aplicacions Biomèdiques de la RMN (GABRMN)
Departament de Bioquímica i Biologia Molecular (BBM). Unitat de Biociències
Universitat Autònoma de Barcelona (UAB), Cerdanyola del Vallès, Spain

Abstract. The exploration of brain tumours usually requires non-invasive techniques such as Magnetic Resonance Imaging (MRI) or Magnetic Resonance Spectroscopy (MRS). While radiologists are used to interpreting MRI, many of them are not used to the biochemical information provided by MRS. In this situation, radiologists may benefit from the use of computer-based support for their decisions. As part of the development of a medical Decision Support System (DSS), MRS data corresponding to various tumour pathologies are used to assist expert diagnosis. The high dimensionality of the data might obscure peculiarities and anomalies that would jeopardize automated DSS diagnostic assistance. We illustrate how visualization, combined with expert opinion, can be used to explore data in a process that should improve computer-based tumour classification.

1 Introduction

Diagnostic decision making in oncology is always a sensitive matter, and even more so in the specific area of brain tumour oncology, for which the direct and indirect costs - both human and financial - of misdiagnosis are very high. Medical experts often take decisions on the basis of prior knowledge gleaned from their experience but, in this context, in which most diagnostic techniques must be non-invasive, clinicians should benefit from the use of an at least partially automated computer-based DSS.

AIDTumour (Artificial Intelligence Decision Tools for Tumour diagnosis) is a research project for the design and implementation of a medical DSS to assist experts in the diagnosis of human brain tumours on the basis of data obtained

*Alfredo Vellido is a Ramón y Cajal researcher. The authors acknowledge funding from Spanish MEC projects TIN2006-08114 and SAF2005-03650. Authors gratefully acknowledge the former INTERPRET partners (INTERPRET, EU-IST-1999-10310) and, from 1st January 2003, Generalitat de Catalunya (grants CIRIT SGR2001-194, XT 2002-48 and XT 2004-51); data providers: Dr. C. Majós (IDI), Dr.À. Moreno-Torres (CDP), Dr. F.A. Howe and Prof. J. Griffiths (SGUL), Prof. A. Heerschap (RU), Dr. W. Gajewicz (MUL) and Dr. J. Calvar (FLENI) ; data curators: Dr. A.P. Candiota, Ms. T. Delgado, Ms. J. Martín, Mr. I. Olier and Mr. A. Pérez (all from GABRMN-UAB); GABRMN group leader: Prof. Carles Arús.

by MRS. This is a technique that can shed light on cases that remain ambiguous after clinical investigation. The MRS data used in AIDTumour and analyzed in this brief paper belong to a complex multi-centre set containing cases of several brain tumour pathologies diagnosed by biopsy and characterised according to the World Health Organization (WHO) classification system. These data have undergone a rigorous pre-processing quality control [1] that fully validates them from the point of view of the radiologists. Nevertheless, and from the viewpoint of their use in an automated computer-based DSS, the various origins of these spectra and the complexity of their pre-processing make further data exploration advisable. It might be problematic to include some data cases straightforwardly in an automated DSS for three different reasons: Firstly, some may contain measurement or acquisition artefacts that, even if not completely precluding diagnosis by visual inspection, might induce errors in computer-based diagnosis. Secondly, atypical cases, even if not containing artefacts: would be classed as outliers [2]. Thirdly, some cases with a clear biopsy-based diagnosis may have spectra that are quantitatively similar to those of other tumour types. An expert radiologist would still classify them correctly by visual inspection, but they may mislead a computer-based automated classification system.

The aforementioned cases are bound to be problematic for they are likely to unduly bias the automated classification process in the DSS, even if for different reasons. The MRS dataset used in AIDTumour has already been classified in the past using simple linear techniques such as Linear Discriminant Analysis [3] or more sophisticated machine learning non-linear techniques such as Support Vector Machines [4]. Nevertheless, and to the best of the authors' knowledge, the potential problems outlined above have never been taken into consideration prior to classification. In this paper, we show the effectiveness of a method to identify and characterize potentially conflicting MRS data that combines techniques of dimensionality reduction and exploratory visualization with expert knowledge. This method is conceived as a preliminary step to data classification. Dimensionality reduction is not trivial in this setting, as the available MRS data are scarce and high dimensional. Sammon's mapping is used to this end.

2 MRS Brain tumour dataset

The data analysed in AIDTumour correspond to 304 single voxel short echo time ^1H MR spectra acquired in vivo from brain tumour patients, out of which 217 are used in this study, including: meningiomas (58 cases), glioblastomas (86), metastases (38), astrocytomas Grade II (22), oligoastrocytomas Grade II (6), and oligodendrogliomas Grade II (7). For details on data acquisition and processing, see [1]. Class labelling was performed according to the World Health Organization (WHO) system for diagnosing brain tumours by histopathological analysis of a biopsy sample. For the reported analysis, spectra were grouped into three superclasses: high grade malignant tumours (metastases and glioblastomas), low grade gliomas (astrocytomas, oligodendrogliomas and oligoastrocytomas) and meningiomas. The clinically-relevant regions of the spectra were

sampled to obtain 195 frequency intensity values (data attributes), from 4.25 parts per million (ppm) down to 0.56 ppm.

3 Methods

As mentioned in the introduction and in section 2, the available MRS data have high dimensionality. This makes dimensionality reduction for visual exploration a non-trivial undertaking. In order to allow the visualization of the data, the spectra are mapped onto a 3-D space through Sammon’s mapping [5] expressed as an implicit function $f: \mathbb{R}^{195} \rightarrow \mathbb{R}^3$, where 195 is the number of frequency intensity variables. The non-linear mapping is constructed as to minimize the interpoint distortions it introduces, which is quantified by Sammon’s error measure:

$$\text{Sammon's Error} = \frac{1}{\sum_{i < j} \delta_{ij}} \frac{(\sum_{i < j} \delta_{ij} - \xi_{ij})^2}{\delta_{ij}}$$

where δ_{ij} is a dissimilarity measure (the Euclidean distance in our study) between any spectra i and j in the original data space and ξ_{ij} is the Euclidean distance between the images of spectra i and j under function f in the 3-D space. In this study, the minimization of the Sammon’s error was performed by the Newton method for optimization. A collection of models was obtained by varying the initial points (100 different random values) and the step size (9 different values), for a total of 900 runs. The model with lowest Sammon’s error (0.018) was selected for further analysis. An NMR expert is then confronted with the visualization of Sammon’s mapping of the spectra, created in this study with the free software package KING (kinemage.biochem.duke.edu/software/king.php). The expert singles out those spectra she/he considers to be potentially conflictive - according to the modalities outlined in the introduction - and compares them to the characteristic spectra that correspond to their tumour type. If artefacts are found, the spectrum is tagged with information about their causes and recommendations on the suitability of its use for classification are made. If the spectrum is found to be an outlier, it is tagged as such. If it is a potentially conflicting case for an automated classifier, a warning is included in the tag.

4 Experimental results and discussion

A 3-D snapshot of the data mapping obtained using Sammon’s method is visualized in Figure 1. High grade malignant tumours are displayed in black, low grade gliomas in white, and meningiomas in gray. Overall, these three groups look well-defined and show a reasonable degree of separation, but it is also clear that some cases do not conform to this behaviour and that some of the issues outlined in the introduction should be considered.

Some cases appear to be atypical. It is impossible to discern *a priori* if this is due to measurement or processing artefacts or if, alternatively, these are correct but unusual cases, or outliers. The NMR expert, though, can carry out such disambiguation. Quite a few cases were identified as artefacts by the expert.

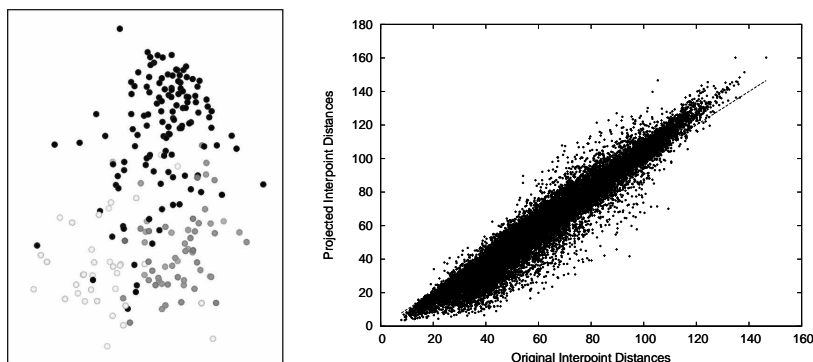


Fig. 1: A 3-D view of the projected MRS data obtained by Sammon’s mapping (left: High grade malignant tumours are displayed in black, low grade gliomas in white, and meningiomas in gray) and the original and projected interpoint distances (right).

For illustration, two of them are listed in Table 1 (top), which also includes the type of informative tag that would be appended to them in a practical implementation of the DSS. Figure 2 (top row) displays a different 3-D view of the data with these two cases highlighted and linked to their spectra, neatly different to the average of their tumour type group.

Some other cases were identified by the expert as atypical, even though not including artefacts. Two of them are listed in Table 1 (middle), which also includes the type of informative tag that would be appended to them in a practical implementation of the DSS. They are visualized in Figure 2 (middle row)

Finally, some cases, although not data outliers, are potentially problematic for inclusion in a computer-based automated classification process. Three of those identified by the expert are listed in Table 1 (bottom), together with their corresponding informative tag. They are visualized in Figure 2 (bottom row)

Many other cases conforming to these three categories were found, but their description, as well as its visual representation are skipped because of space limitations. The interactive visualization of the data mapping and the expert textual comments and recommendations are meant to be integrated in the AIDTumour DSS. Future research will address the automatic quantification of the number and extent of data outliers and the expert tagging of potentially ambiguous cases that reside on the borders between tumour classes.

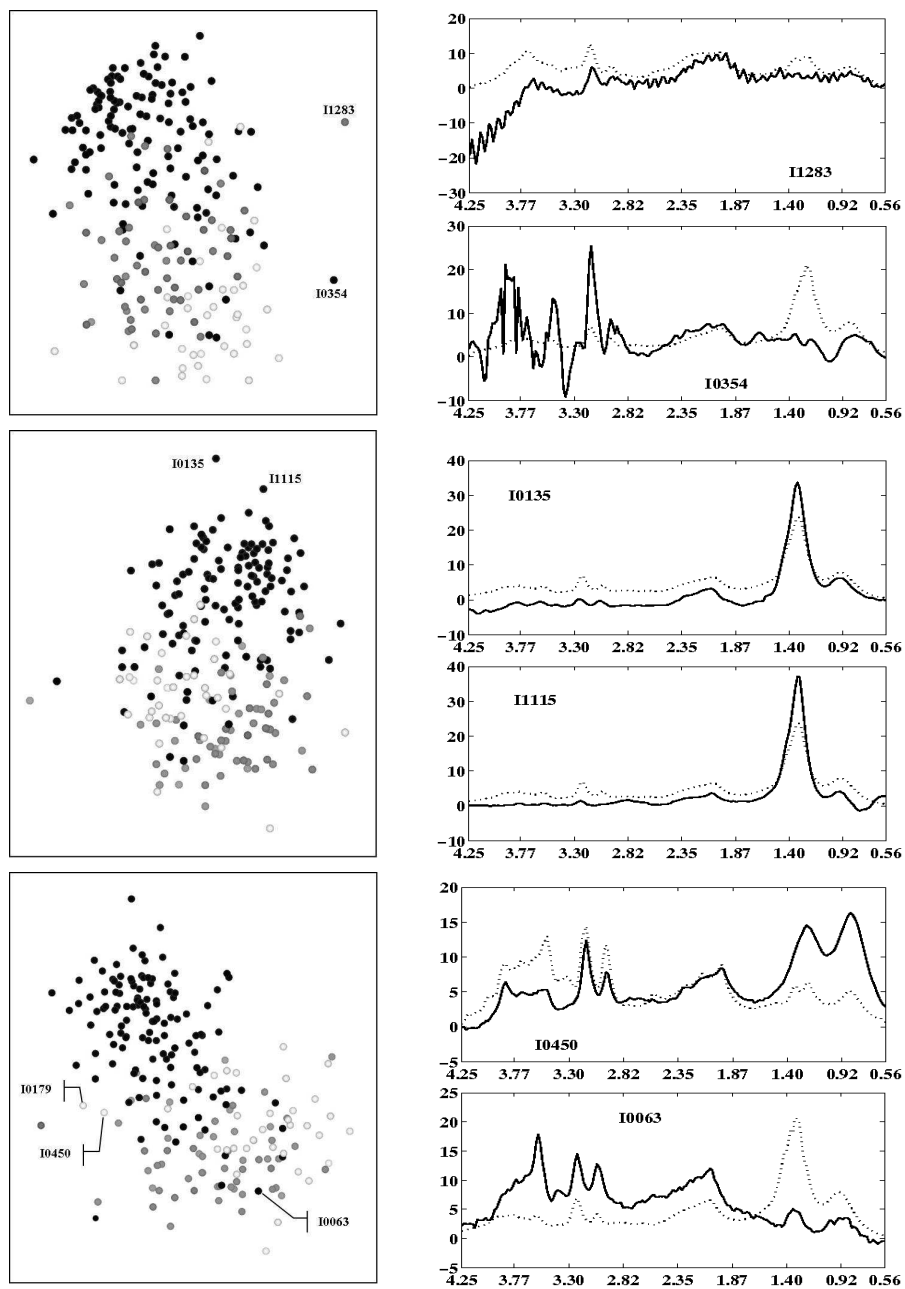


Fig. 2: 3-D views of several cases of interest (left column) and their corresponding individual spectra (solid line) and mean spectra of the superclasses they belong to (dotted line). The abscissa axis displays frequency in ppm.

CASE	TAG	RECOMM.
I1283	This spectrum of a meningioma shows an artefact produced by a phenomenon called eddy currents upon acquisition of the data. An expert spectroscopist would still be able to classify it.	Remove it from the dataset in classification tasks.
I0354	This glioblastoma shows a possible “polispiculated artefact”, which does not preclude its interpretation, as most of the important metabolites are not affected by it. It also shows a lack of necrotic lipids, infrequent for this pathology.	Remove it from the dataset in classification tasks.
CASE	TAG	RECOMM.
I1115 and I0135	These two cases (I1115, a metastasis and I0135, a glioblastoma) show an extreme necrotic lipid pattern (high peak at around 1.3 ppm). The signal amplitude ratio 1.3ppm/0.9ppm is much higher (approx. 7 to 1) than that for the average metastasis or glioblastoma (approx. 3 to 1).	This outlier might skew overall class definition, as well as bias cluster analysis.
CASE	TAG	RECOMM.
I0179 and I0450	Low-grade glial tumours located in the high-grade malignant region. They display an unusual pattern of mobile lipids, with peaks at 0.8 and 1.3ppm as in high-grade malignant tumors, but in contrast to them, the 0.8 ppm peak is of the same magnitude as the 1.3 ppm peak.	Beware a possible misclassification by the DSS automated algorithm.
I0063	This spectrum of a glioblastoma has an MRS pattern that is undistinguishable from that of a typical low-grade glial tumour. The spectral pattern is an infrequent one for a glioblastoma, although not completely unknown.	Beware a possible misclassification by the DSS automated algorithm.

Table 1: Spectra that are either affected by artefacts (top table), might be considered outliers (middle), or potentially conflictive for DSS classification (bottom).

References

- [1] M. Julià-Sapé et al. A multi-centre, web-accessible and quality control-checked database of in vivo MR spectra of brain tumour patients. *Magn. Reson. Mater. Phy.*, 19:22-33, 2006.
- [2] A. Vellido and P.J.G. Lisboa, Handling outliers in brain tumour MRS data analysis through robust topographic mapping, *Comput. Biol. Med.*, 36:1049-1063, 2006.
- [3] A.R. Tate et al., Automated classification of short echo time in vivo ^1H brain tumor spectra: a multicenter study, *Magn. Reson. Med.* 49: 29-36, 2003.
- [4] A. Devos et al., Classification of brain tumours using short echo time ^1H MR spectra, *J. Magn. Reson.*, 170:164-175, 2004.
- [5] J.W. Sammon Jr, A nonlinear mapping for data structure analysis, *IEEE T. Comput.*, C-18:401-409, 1969.